Measurement in a wind tunnel of dry deposition velocities of submicron aerosol with associated turbulence onto rough and smooth urban surfaces

Pierre Roupsard, Muriel Amielh, Didier Maro, Alexis Coppalle, Hubert Branger, Olivier Connan, P. Laguionie, D. Hébert, M. Talbaut

Elsevier Editorial System(tm) for Journal of Aerosol Science
Manuscript Draft

Manuscript Number:

Title: MEASUREMENT IN A WIND TUNNEL OF DRY DEPOSITION VELOCITIES OF SUBMICRON AEROSOL WITH ASSOCIATED TURBULENCE ONTO ROUGH AND SMOOTH URBAN SURFACES

Article Type: Regular Paper

Keywords: dry deposition; deposition velocity; submicron aerosol; urban surfaces; wind tunnel

Corresponding Author: Mr. Pierre Roupsard, M.D.

Corresponding Author's Institution: IRSN

First Author: Pierre Roupsard, M.D.

Order of Authors: Pierre Roupsard, M.D.; Muriel Amielh, PhD; Denis Maro, Professor; Alexis Coppalle, Professor; Hubert Branger, PhD; Olivier Connan, PhD; Philippe Laguionie, PhD; Didier Hébert; Martine Talbaut, PhD

Cover Letter

Please find as attached files a manuscript untitled:

“Measurement in a wind tunnel of dry deposition velocities of submicron aerosol with associated turbulence onto rough and smooth urban surfaces”,

co-authored by : P. Roupsard, M. Amielh, D. Maro, A. Coppalle, H. Branger, O. Connan, P. Laguionie, D. Hébert and M. Talbaut; for submission to “Journal of Aerosol Science”.

Best regards.

Pierre Roupsard

HIGHLIGHTS:

- Submicron aerosol deposition on urban surfaces is studied in a wind tunnel.
- Associated turbulent parameters are measured or estimated with a hot wire anemometry.
- Settling has an influence on deposition on smooth surface and at low wind speed.
- Submicron aerosol deposition is dependent on turbulent deposition processes.

MEASUREMENT IN A WIND TUNNEL OF DRY DEPOSITION VELOCITIES OF SUBMICRON AEROSOL WITH ASSOCIATED TURBULENCE ONTO ROUGH AND SMOOTH URBAN SURFACES

P. Roupsard[1*], M. Amielh[2], D. Maro[1], A. Coppalle[3], H. Branger[2], O. Connan[1], P. Laguionie[1], D. Hébert[1] and M. Talbaut[3].

[1]Laboratoire de Radioécologie de Cherbourg-Octeville (LRC), Institut de Radioprotection et de Sûreté Nucléaire (IRSN), 50130 Cherbourg-Octeville, France.

pierre.roupsard@irsn.fr; denis.maro@irsn.fr; olivier.connan@irsn.fr; philippe.laguionie@irsn.fr; didier.hebert@irsn.fr

[2]Institut de Recherche sur les Phénomènes Hors Equilibre (IRPHE), CNRS, UMR-7342, 13384 Marseille, France.

amielh@irphe.univ-mrs.fr; branger@irphe.univ-mrs.fr

[3]Complexe de Recherche Interprofessionnel en Aérothermochimie (CORIA), UMR-6614, 76801 Saint-Etienne du Rouvray, France.

alexis.coppalle@coria.fr; martine.talbaut@coria.fr

*CORRESPONDING AUTHOR: pierre.roupsard@irsn.fr

Tel +33 2 33 01 41 00

Fax +33 2 33 01 41 30

Laboratoire de Radioécologie de Cherbourg-Octeville

Rue Max-Pol Fouchet

50130 Cherbourg-Octeville, France

ABSTRACT:

In the event of accidental discharges of radionuclides in particulate form by a nuclear plant, dry deposition is the only transfer pathway under dry atmospheric conditions. In this case, for the urban environment, these deposits must be assessed precisely in the urban canopy to estimate the doses potentially received by the population. The objectives of this wind tunnel study are to measure dry deposition velocities of a submicron fluorescein aerosol onto horizontal and vertical urban surfaces of glass, cement facing and grass for several wind speeds and to measure the turbulence parameters associated with these deposition velocities. These deposition velocities are then compared to data of the literature and to the

results of two models for dry deposition. The dry deposition velocity of the fluorescein aerosol increases with the intensity of the turbulence. This highlights the importance of the turbulent processes of impaction and interception in deposition. However, the ratio of dry deposition velocity to friction velocity depends on the surface type. It depends on the turbulence conditions in the boundary layer. These turbulent dry deposition processes thus vary in importance depending on the studied surface. Finally, settling represents a significant part of the deposition for low wind speeds and for smooth surfaces. This wind tunnel study permits the study of the deposition as a function of turbulent processes. It should be supplemented by *in situ* experiments to take into account all the physical processes involved under real conditions.

KEYWORDS: Dry Deposition, Deposition Velocity, Submicron Aerosol, Urban Surfaces, Wind Tunnel.

I. Introduction

In a polluted atmosphere or during transit of a plume containing stable or radioactive pollutants, and in the absence of rainfall events, dry deposition is the only transfer pathway from the air to the surface for particles and pollutants. At present, this dry deposition has been studied especially on natural surfaces representing the first link in the human food chain, but very little in the urban environment (Kelly, 1987; Fowler *et al.*, 2009). However, a significant portion of the human population is concentrated in the urban environment, and in the case of passage of a radioactive plume, the quantity of radionuclides deposited by aerosols must be taken into account in estimating the dose rates received by the population (Kelly, 1987). Precise assessment of the transfer of pollutants by dry deposition of aerosols can thus be very important, and the lack of significant data for the urban environment is now acknowledged. Dry deposition of aerosols depends on the aerosol diameter, the deposition surface (the roughness and temperature, for example) and the turbulence conditions (Sehmel, 1980). Therefore aerosols do not deposit homogeneously in the urban environment. In the case of radioactive pollutants, this deposition must be studied for various surfaces, on a wall or street level, and not for an urban canopy, on a neighbourhood or city level, because the distribution of the deposits must be known precisely to assess the doses received by the residents. The dry deposition velocity is the coefficient used to quantify the transfer of aerosol particles by dry deposition in the environment. Most of the measurements of dry deposition velocities on urban surfaces in urban environments were conducted by Roed (1983, 1985, 1987) as a result of the fallout from nuclear tests and the Chernobyl accident, and by Pesava *et al.* (1999) and Maro *et al.* (2010) with a tracer aerosol generated *in situ*. However, these deposition velocities are not associated with precise measurements of turbulence or local meteorology. Presently, there are very few experimental data related to turbulent parameters for urban environments and surfaces. As a result there are significant uncertainties in the use of predictive models of deposition for this environment (Fowler *et al.*, 2009). Urban environments are complex and heterogeneous from the point of view of the turbulence and measurements under simple conditions should aid in understanding the deposition processes and quantifying deposition velocities on urban surfaces. The wind tunnel is an advantageous tool. It can be used as an initial approach to quantifying dry deposition velocities as a function of a restricted number of controlled parameters and reproducible experiments can be conducted. Dry deposition has already been the subject of wind tunnel studies, on natural surfaces (Chamberlain, 1967) or on smooth and rough substrates (Liu and Agarwal, 1974; Horvath *et al.*, 1996; Toprak *et al.*, 1997; Dai *et al.*, 2001), but rather for micron particles. However, the accumulation mode of the atmospheric aerosol (0.1 µm ≤ d_p ≤ 1 µm) is

the mode that is the primary vector for chemical pollutants and radionuclides. It is the mode on which the surface distribution of the atmospheric aerosol is centred (Gründel and Porstendörfer, 2004; Van Dingenen *et al.*, 2004; Papastefanou, 2008). Moreover, it transports these pollutants over large distances from a source to the urban environments, due to a relatively long residence time in the atmosphere (Jaenicke, 1988; Papastefanou, 2006). While the deposition of particles greater than a micrometre most often studied is strongly affected by sedimentation, deposition of submicron aerosols, which are less studied, results from the contribution of several physical processes (Brownian diffusion, impaction, interception). The main objective of this study is to quantify dry deposition velocities of a submicron aerosol on horizontal and vertical urban surfaces, for several wind speeds and under isothermal conditions in the wind tunnel. Various turbulent boundary layer conditions are thus encountered. These turbulence conditions associated with the dry deposition velocities are quantified by hot wire anemometer measurements and focus especially on determination of the friction velocities. Finally, the data from this study are compared to data in the literature and to operational models, solved analytically, developed for smooth surfaces (Lai and Nazaroff, 2000) and natural canopies (Zhang *et al.*, 2001).

II. Experimental setup

II.1 The wind tunnel and the studied surfaces

The experiments were conducted in a recirculating wind tunnel of the IRPHE (University of Aix-Marseille, campus of Luminy, Marseille, France). The experimental test section is a glass channel with a stainless steel base 8650 mm long and a cross-section 280 mm high and 640 mm width. Airflow speeds between 0.5 and 19 m s^{-1} can be generated. Deposition was studied on horizontal conventional glass surfaces, cement facing and synthetic grass in a first experimental campaign (Fig. 1.a), then on vertical conventional glass and cement facing surfaces in a second campaign (Fig. 1.b). The commercial names of the materials and the roughness parameters of the cement facing (Flori *et al.*, 2007) and synthetic grass are listed in Table 1. The roughness parameters of the cement facing measured by laser roughness measurements are the arithmetic mean deviation of the profile Ra, the standard deviation of the profile Rq, the valley depth of the profile Rv and the peak height of the profile Rp. The synthetic grass is composed of primary straight blades grouped into tufts, and thinner and shorter curly blades included in the canopy to make it denser. The parameters characterising the synthetic grass were determined by the authors for the primary straight blades and are the average canopy height h_c, the length of the straight blades l_b, the width of these blades w_b, the number of tufts per square metre n_t and the number of straight blades per

105 square metre n_b. During the experiments on horizontal surfaces, the bottom of the test section was
106 successively completely covered by each type of surface to develop the boundary layers and turbulence
107 conditions characteristic of each surface.

108 Table 1: characteristics of the studied surfaces.

	Conventional glass	**Cement facing**	**Synthetic grass**
Commercial name	*Planilux*®, Saint-Gobain	Fema®-*Therm-Mineralputz* 5 mm	"*Romana*"
Roughness parameters	Glass thickness = 4 mm	Ra = 0.57 mm	h_c = 34 ± 2 mm
		Rq = 0.74 mm	l_b = 38.4 ± 1.9 mm
		Rv = 2.36 mm	w_b = 1.2 ± 0.1 mm
		Rp = 1.86 mm	n_t = 10364 m^{-2}
			n_b = 164675 m^{-2}

109

110 In the same way, a vertical wall of the test section was successively covered with conventional glass and
111 cement facing, to measure deposition on a vertical wall. It should be noted that glass cover the walls in
112 the form of a pavement of square plates 200 mm on a side, while the cement facing and synthetic grass
113 covered the wind tunnel homogeneously and continuously. To study deposition over a broad range of
114 wind speeds that can be encountered in the urban environments, airflows of speeds u_{ref} of 1.3, 5.0 and
115 9.9 m s^{-1} were generated in the test section. The turbulence was quantified above all the horizontal
116 surfaces.

117 ***II.2 Quantification of the dry deposition velocity*** V_d

118 The dry deposition velocity V_d (m s^{-1}) of an aerosol is defined by Chamberlain and Chadwick (1953, in
119 Sehmel, 1980) as the ratio of the surface flux of dry deposition F (kg m^{-2} s^{-1}; by convention a deposition
120 flux is negative) by the average concentration of the aerosol in the air C (kg m^{-3}) at a given height (1).

$$V_d = \frac{-F}{C} \quad (1)$$

121 A common approach to measure dry deposition velocities is to use a stable or radioactive chemical tracer
122 for the studied aerosol. This method has the advantage of directly measuring a quantity of tracer, and
123 thus of particles, in number or in mass. The deposition flux F is calculated according to (2), $M_{substrate}$ (kg) is
124 the mass of tracer, $A_{substrate}$ (m^2) is the total surface of the substrate sample, and t (s) is the duration of the
125 experiment.

$$-F = \frac{M_{substrate}}{A_{substrate}\, t} \quad (2)$$

The average concentration C is calculated according to (3), with M_{filter} (kg) the mass of tracer collected on the filter with an airflow rate Q_{filter} ($m^3\ s^{-1}$) over the same duration t.

$$C = \frac{M_{filter}}{Q_{filter}\, t} \quad (3)$$

A slightly polydispersed monomodal submicron dry fluorescein aerosol (uranine, ρ = 1500 kg m^{-3}) generated with a pneumatic generator is used as a tracer. The operating principle of this generator is described in French standard NF X 44-011. A fluorescein solution is nebulised, the produced droplets are sorted by centripetal filters, then entrained and dried by a dry air flow to obtain a dry solid fluorescein aerosol. The granulometric mass distribution of this aerosol was measured by three samplings with a Dekati (LPI) low pressure cascade impactor (separation of the particles over 12 stages of cutoff diameters between 24 nm and 9.55 µm) and gave on average an aerodynamic mass median diameter d_{amm} of 0.27 ± 0.07 µm with a geometric standard deviation of 2.06 ± 0.23 (Fig. 2). The air recirculation in the wind tunnel allows to generate particles only for the first two minutes of the experiment and to let the concentration to decrease with time until the end of the experiment. Substrate samples are removed at the end of the fifteen minutes of the experiment. The generated aerosol is introduced at the outlet of the test section to be mixed with air in the recirculation section of the wind tunnel so that its concentration will be homogeneous over the test section inlet. It is injected at the centre of the cross-section with a horizontal copper injection nozzle regularly pierced along a line oriented toward the outlet duct with an airflow rate of 10.8 $m^3\ h^{-1}$. Finally, the air in the test section is renewed between experiments by extracting air towards the exterior. The dry deposition fluxes are measured by exposure of samples (square plates 200 mm on a side composed of the studied substrates) to the fluorescein aerosols for a the experiment time. Samples are used for several experiments. After they are rinsed with distilled water and dried at room temperature, the substrates are placed in the test section with great care so as not to pollute them with fluorescein deposited on the walls of the test section. The static electrical charge is consistently removed from the synthetic grass samples by spraying the blades with denatured ethanol. The charge state of these specimens is then checked with a fieldmeter (Eltex EMF 58). During the experiments on horizontal substrates, three rows of three samples placed across the width of the test section are incorporated into the substrate studied at various distances from the test section inlet. These distances from the inlet are also called “fetch” (m). The edges of these specimens adjoin the substrate surfaces covering the base of the test section. The leading edges of each row of samples are located at

1.0, 5.0 and 6.8 m from the inlet. Each type of substrate is studied separately, as the base of the section is completely covered by a single type of substrate. To measure dry deposition velocities on vertical surfaces, the vertical wall used is covered in the same way with the studied substrate, from the test section inlet to 6 m inside the test section. Three samples are intercalated lengthwise into this vertical wall, with leading edges at 4.8, 5.0 and 5.2 m, to measure the dry deposition fluxes. These specimens are centred in height, 40 mm from the base of the test section. In parallel, samples are taken on cellulose filters (Whatman 1440-047) throughout the exposure time of the specimens to the aerosol in order to quantify its concentration in the air of the test section. Bent copper sampling tubes with a 10 mm inside diameter are introduced from the top of the section so as not to perturb the flow above the studied surfaces and connected to filter holders with 500 mm long fluoroelastomer tubing. During the experiments on horizontal substrates, three samples are taken on filters 10 mm above the surface halfway across the test section, downstream of the specimens, with the inlet of the tube just behind each row of samples (fetch = 1.2, 5.2 and 7.0 m) so as not to perturb the flow over the specimens and thus not to perturb deposition. Likewise, for the experiments on vertical substrates, a sample is taken on a filter just behind the third specimen, 10 mm from the wall, halfway up the test section. In each experiment, a sample is taken on a filter at the centre of the test section, 5.2 m from its entrance, to control *a posteriori* the homogeneity of the particle concentration in the air in the section during the experiment. Collection flow rates are between 7.6 and 8.6 L min^{-1} and are checked with a TSI *4000 Series* mass flowmeter. The samples and filters are carefully removed, wrapped in aluminium foil to avoid any pollution, and then treated for measurement. Fluorescein is hydrophilic, thus the deposited particles are dissolved simply by rinsing the surface with a pH 9 solution of ammonia water using a syringe (with successive rinsings with the same solution for the glass and cement facing) or directly by soaking (synthetic grass). The filters are immersed directly in the ammonia water to dissolve the filtered fluorescein particles. These solutions are measured with a fluorescence spectrometer (Jobin Yvon Horiba FluoroMax-3) to determine $M_{substrate}$ and M_{filter}. The background fluorescence of each type of surface is subtracted from the measurement result. Experiments are conducted at least twice to ensure their repeatability.

II.3 Estimation of the turbulent parameters

In the wind tunnel, in the absence of heat exchange on the studied surface, the turbulent parameter mainly associated with V_d is the friction velocity u_* (m s^{-1}) because it quantify mechanical turbulence that enhance the aerosol deposition. Also, it is one of the parameters necessary in modelling V_d in confined environments (Lai and Nazaroff, 2000) or *in situ* (Zhang *et al.*, 2001). It quantifies the turbulence

generated by shear of a flow over a surface and is used as a reference velocity near the wall. The friction velocity is estimated with (4) by measuring τ_p (kg m^{-1} s^{-2}), the frictional or shear stress at the wall, with ρ (kg m^{-3}) the fluid density.

$$u_* = \sqrt{\frac{\tau_p}{\rho}} \tag{4}$$

It can also be estimated with (5) using velocity profile measurements above the surface.

$$\frac{u(z)}{u_*} = \frac{1}{\kappa} \ln \frac{z-d}{z_0} \tag{5}$$

$$\frac{u(z)}{u_*} = \frac{1}{\kappa} \ln \frac{z-d}{k_s} + B \tag{6}$$

In (5), $u(z)$ (m s^{-1}) is the mean velocity in the flow direction measured at the vertical position z (m), and κ (0.4), d (m) and z_0 (m) are respectively the Von Karman constant, the displacement height and the aerodynamic roughness height. The friction velocity can be estimated by fitting this relation in the logarithmic overlap area of the velocity profile of a developed turbulent boundary layer; u_*, d and z_0 are then the parameters to be fitted. The aerodynamic roughness height is flow-dependent for dynamically smooth flows and depends on roughness geometry for fully rough flows (Raupach *et al.*, 1991). For synthetic grass, z_0 is equal to $0.13h_c$ (Tanner and Pelton, 1960, Stanhill, 1969 in Raupach *et al.*, 1991). For cement facing, z_0, is determined from (5) and (6), and equal to $k_s \exp(-B\kappa)$ (B = 8.5; Schlichting, 1968), with $k_s = Rv + Rp$. For glass, d is equal to zero and z_0 can vary. The relative turbulence intensity I (%) is another dimensionless magnitude that quantifies the turbulent agitation (u', w') of a flow by comparison to the average motion ($\bar{u}$) at a distance z from the wall. The relative turbulence intensities for the components u and w (I_u and I_w) can be calculated according to (7.a) and (7.b).

$$I_u = \frac{\sqrt{\overline{u'^2}}}{\bar{u}} \; ; \; I_w = \frac{\sqrt{\overline{w'^2}}}{\bar{u}} \tag{7.a); (7.b)}$$

With this magnitude, turbulence can be classified into three categories: low (1%), medium (10%) and high (20% and more). The turbulent parameters were estimated in absence of aerosol injection for horizontal surfaces using hot-wire anemometry operating at high frequency. The system used is a probe with two crossed hot wires (type 55P61) combined with a *Streamline* anemometry system (Dantec Dynamics). It measures u, the horizontal component of velocity in the flow direction, and w, the vertical component, at high frequencies (2.5 kHz for u_{ref} = 1.3 m s^{-1} and 10 kHz for u_{ref} = 5.0 and 9.9 m s^{-1}, u_{ref} measured at the center of the test section of the wind tunnel) with a 50 seconds acquisition duration in each position.

These turbulence measurements were conducted above each surface type for each u_{ref} and for each fetch above the centre of the central substrate sample, by vertical profiles of 40 points between z = 2.5 mm and z = 200 mm above the roughnesses of the surfaces.

III. Results and discussions

III.1 Dry deposition velocities V_d

The measured concentrations of aerosols in the air show no significant difference between the sample in the centre of the test section and samples 10 mm from the walls during the experiments (median deviation of 6.6%) and show homogenisation of the aerosol concentration in the air recirculation circuit of the wind tunnel. The average dry deposition velocities on each type of horizontal surface are calculated from the deposition fluxes at 1.0, 5.0 and 6.8 m from the test section inlet and the associated concentrations for each flow speed. They show neither variation with the fetch, nor a notable difference between the specimens at the centre of the row and those on the sides. The average dry deposition velocities calculated for each type of surface, horizontal and vertical, and for each airflow speed u_{ref} are shown in Table 2 and Fig. 3. The dry deposition velocities measured on horizontal surfaces vary from 1.2 10^{-5} m s^{-1} on conventional glass for u_{ref} = 1.3 m s^{-1}, to 1.4 10^{-3} m s^{-1} on synthetic grass for u_{ref} = 9.9 m s^{-1}. Thus there is a factor of over two orders of magnitude between the lowest and highest values measured on these urban surfaces.

Table 2: average V_d as a function of u_{ref}.

u_{ref} (m s^{-1})	V_d (x 10^{-5} m s^{-1})				
	Glass		Cement facing		Synthetic grass
	Horizontal	Vertical	Horizontal	Vertical	
1.3	1.4 ± 0.4		2.2 ± 0.9	1.4 ± 0.3	28.1 ± 8.4
5.0	2.3 ± 1.3	1.1 ± 0.4	4.8 ± 1.8	3.6 ± 0.7	54.6 ± 19.3
9.9	4.5 ± 2.0	2.4 ± 0.3	7.2 ± 1.6	8.0 ± 2.0	124.7 ± 29.6

Those measured on vertical surfaces vary from 1.1 10^{-5} m s^{-1} on conventional glass for u_{ref} = 5.0 m s^{-1} to 8.0 10^{-5} m s^{-1} on cement facing for u_{ref} = 9.9 m s^{-1}. The dry deposition velocity V_d could not be measured on vertical conventional glass for u_{ref} = 1.3 m s^{-1} during the experimental campaign.

III.2 Turbulent parameters

Aerodynamic parameters determined by hot wire measurements are listed in Table 3. All the developed boundary layers are turbulent at fetches of 1.1, 5.1 and 6.9 m, with a transition zone to the logarithmic profile (Fig. 4). The friction velocities are determined by fitting the logarithmic relation (5) to the mean velocity profiles. The estimated friction velocities decrease for an increasing fetch. This variation is consistent with the reduction in the stress at the wall τ_p upon development of a completely turbulent boundary layer (Antonia and Luxton, 1971). The representation of the profiles in terms of dimensionless velocity $(u + \Delta u)+$ and dimensionless vertical position $(z + d)+$ ($u+ = u / u_*$; $z+ = z\, u_* / \nu$, with ν the kinematic viscosity of air) and the mean velocity shifts values Δu, with $\Delta u = \ln z_0+ + C$ ($C = 5$), show the different rough regimes of the flows generated by each surface type at each u_{ref} (Krogstad and Antonia, 1999).

The profiles of I_u and I_w were calculated using (7.a) and (7.b), and profiles of I_w are shown in Fig. 5. All the profiles over u and w have the same shape, with a maximum I_{wmax} in the immediate vicinity of the surface. The calculated values are shown in Table 3. For equal u_{ref}, the values of I_{umax} and I_{wmax} are higher for synthetic grass than for cement facing, and higher for cement facing than for glass, with I_{umax} greater than I_{wmax}. These observations are consistent with the observations of Antonia and Luxton (1971) for a boundary layer on a rough surface. Unlike the friction velocities, these relative turbulence intensities show no notable decrease as a function of the fetch but are essentially constant at each fetch for the same surface at the same flow speed.

III.3 Discussions

The average deposition velocities for each type of surface and each u_{ref} (Table 2) have been compared to the data of the literature (Fig. 6). The deposition velocities measured in this study are of the same order of magnitude as those in the literature for smooth surfaces and grass. The absence of data on the geometry of the surface roughnesses studied by Toprak et al. (1997) makes it impossible to understand the differences in the measured V_d. The dry deposition velocities vary with the mean air flow speed, the surface type and the orientation of the surface. On horizontal surfaces, V_d varies on average by a factor of 1.7 and 23.7 respectively between conventional glass and cement facing and between conventional glass and synthetic grass, and by a factor of 1.9 and 3.6 between $u_{ref} = 1.3$ m s^{-1} and $u_{ref} = 5.0$ m s^{-1} and between $u_{ref} = 1.3$ m s^{-1} and $u_{ref} = 9.9$ m s^{-1} respectively.

Table 3: aerodynamic parameters for each surface as a function of u_{ref} and the fetch.

		Conventional glass					Cement facing						Synthetic grass					
Fetch (m)	**u_{ref} (m s^{-1})**	**V_d (10^{-4} m s^{-1})**	**u_* (m s^{-1})**	**z_0 (10^{-2} mm)**	***I_{umax} (%)***	***I_{wmax} (%)***	**V_d (10^{-4} m s^{-1})**	**u_* (m s^{-1})**	**z_0 (10^{-2} mm)**	**d (mm)**	***I_{umax} (%)***	***I_{wmax} (%)***	**V_d (10^{-4} m s^{-1})**	**u_* (m s^{-1})**	**z_0 (mm)**	**d (mm)**	***I_{umax} (%)***	***I_{wmax} (%)***
1.1		1.7					3.1						3.3	0.17	4.4	23.9	38.3	18.7
5.1	1.3	1.2	0.06	8.5	25.4	7.2	1.9	0.07	0.1	5.6	25.8	7.4	2.6	0.13	4.4	20.9	33.5	14.9
6.9		1.1	0.06	8.7	24.7	7.5	1.8	0.07	0.1	4.5	26.8	7.0	2.6	0.13	4.4	16.1	35.3	16.6
1.1		2.8	0.26	9.9	23.6	10.1	4.9	0.33	0.1	6.4	21.2	11.0	7.0	0.67	4.4	24.0	44.7	23.7
5.1	5.0	1.4	0.23	4.2	21.2	8.7	4.3	0.29	0.1	4.0	24.3	10.1	5.8	0.52	4.4	17.6	47.6	24.9
6.9		2.2	0.20	1.9	21.2	8.1	5.2	0.27	0.1	2.5	24.0	10.2	3.9	0.56	4.4	13.1	42.5	23.4
1.1		5.6	0.50	5.9	19.1	9.3	7.6	0.66	0.1	5.1	22.8	11.7	13.1	1.37	4.4	24.0	46.6	26.0
5.1	9.9	2.9	0.46	3.1	18.7	8.6	6.5	0.54	0.1	4.0	23.5	10.5	12.1	1.06	4.4	15.6	44.7	25.6
6.9		6.3	0.38	1.5	16.9	8.9	7.4	0.54	0.1	2.8	25.4	11.2	12.1	1.05	4.4	9.0	44.6	24.8

These results show the importance of turbulent processes of interception and impaction for this size range of particles, dependent respectively on the sizes of the aerosol and the obstacle, and on the Stokes number (itself dependent on the relaxation time of the aerosol, the flow speed and the size of the obstacle). Moreover, the measured differences in deposition velocities between horizontal and vertical walls, conventional glass and cement facing are on the order of the sedimentation velocity for the fluorescein aerosol calculated with (7) from the distribution of Fig 2.

$$V_s = \sum_{i=1}^{12} \frac{d_{pi}^2 g C_{ui} \rho}{18\nu} m_{ni} = 1.10 \pm 0.37\ 10^{-5}\ \mathrm{m\ s^{-1}} \qquad (7)$$

Here, g is the gravitational acceleration (9.81 m s^{-2}), ρ is the density of the particles (1000 kg m^{-3} for aerodynamic diameters determined with a cascade impactor,) C_{ui} is the Cunningham correctional factor for the aerosol of diameter d_{pi} (geometric diameter of stage i of the cascade impactor), ν is the kinematic viscosity of air (1.5 10^{-5} m^2 s^{-1}) and m_{ni} is the fluorescein mass on stage i normalised to the total mass of fluorescein collected on the 12 stages. For low wind speeds, the contribution of sedimentation to deposition of this fluorescein aerosol is therefore non-negligible, contrary to what is usually believed for submicron aerosols. It can double the deposition velocity between a vertical wall and a horizontal wall, or even represent the entire deposit on a smooth horizontal wall for a low wind speed, as for glass with u_{ref} = 1.3 m s^{-1}. It should also be noted that deposition velocities on horizontal and vertical cement facing are approximately equal at u_{ref} = 9.9 m s^{-1}. As the deposition flux depends on the vertical wind speed and its fluctuations, the deposition velocity V_d is shown in Fig. 7 as a function of the maximum relative turbulence intensity over w, I_{wmax}. An increase in deposition flux with turbulence intensity was already observed by Dai *et al.* (2001) for a smooth surface. Our graph shows a variation in V_d as a function of I_{wmax} independent of a particular type of surface. This observation is of interest as it represents V_d as a function of a single turbulent parameter for several surface types.

The parameter usually related to V_d is the friction velocity u_*, as it quantifies the turbulence in a boundary layer. It is one of the main parameters used in the deposition models developed for inside and outside environments. The calculated deposition velocities for the polydispersed fluorescein aerosol with the models of Lai and Nazaroff (2000) and of Zhang *et al.* (2001) (with zero aerodynamic resistance, because the concentration above the surface is consistent with that measured in the centre of the test section), and the data of this study are shown as a function of u_* in Fig. 8. The friction velocities of the vertical surfaces associated with the V_d are those estimated for the same horizontal surfaces and same u_{ref} at the

fetch 5.0 m. The model of Lai and Nazaroff (2000) correctly estimates the deposition velocities on glass for u_* greater than 0.2 m s^{-1}, but seems to overestimate them below this for horizontal glass.

On the other hand, Zhang *et al.* (2001) systematically overestimate V_d on grass by more than a factor of 5. This resistive model uses Brownian diffusion as the principal deposition process for a submicron aerosol deposition on grass and underestimates interception and impaction processes. By comparison, the recent mechanistic model of Petroff *et al.* (2008) accords more importance to interception for this aerosol size range. It is in a better agreement with Chamberlain (1967) data on grass in a wind tunnel for micron and submicron aerosols than Zhang *et al.* (2001). This shows the limits of the operational model of Zhang *et al.* (2001) in assessing V_d on grass precisely, and the need to either improve consideration of turbulent processes in deposition on grass, or to estimate V_d from mechanistic models like that of Petroff *et al.* (2008) that better account for these turbulent processes.

In the literature, dry deposition velocities measured *in situ* are generally normalised to u_*. In this case, the sedimentation velocity V_s (7), a non-turbulent deposition process, must be subtracted from V_d. In recent studies of transfers in natural environments, the ratio of V_d and u_* was found to be independent of the various surfaces studied under neutral and stable conditions and approximately equal to 2.10^{-3} (Damay, 2010; Donateo *et al.*, 2010). On the contrary, in this study, this ratio depends on the type of surface (Fig. 9) and thus on the flow conditions and the structure of the boundary layer. It is therefore determined by the importance of interception and impaction in the deposition process. The ratio is $5.3 \pm 4.1\ 10^{-5}$ for conventional glass, $1.5 \pm 0.6\ 10^{-4}$ for cement facing, and $1.3 \pm 0.3\ 10^{-3}$ for synthetic grass. The experimental results are close to the estimate of the model of Lai and Nazaroff (2000) for glass ($5.0 \pm 0.1\ 10^{-5}$) and the *in situ* values of Damay (2010) on a grassland, $0.8\ 10^{-3}$ and $1.6\ 10^{-3}$ respectively for d_p = 0.20 and 0.32 µm, for synthetic grass.

In the urban canopy, in the urban sub-layer of the atmospheric boundary layer, measurable friction velocity u_* in the boundary layers of the surfaces is not obvious. Use of u_* alone as a turbulent parameter seems thus to be limited in modelling deposition on heterogeneous urban surfaces. As an initial approach, in the context of operational models to give quick estimates of deposition velocities, wind speed in the streets could turn out to be a good parameter, as it is easily measurable or modelled. Empirical parameterisation of V_d as a linear function of u_{ref} for each type of surface according to the data of Table 2 could be a good first approximation.

IV. Conclusions

Presently, there is little experimental data on dry deposition velocities for the urban environment. This wind tunnel study was conducted to measure V_d and the associated turbulent parameters for a polydispersed submicron aerosol on urban surfaces. The deposition velocity V_d was measured on three urban surfaces types, horizontal and vertical, and for three flow speeds u_{ref}, and these data were compared to the data of other authors. These deposition velocities show dependence on both u_{ref} and the type of deposition surface, confirming the importance of the turbulent processes of interception and impaction in deposition for an aerosol of this size. However, sedimentation is responsible for a large part of the deposition for smooth horizontal surfaces and for low u_{ref}. The model of Lai and Nazaroff (2000) correctly estimates V_d on glass, while Zhang *et al.* (2001) substantially overestimate it on grass. Finally, this work reveals that parameterisation of V_d as a function of u_{ref} may be relevant for the urban environment in an operational context.

This wind tunnel study treats only a limited number of parameters and types of surfaces. However, it highlights the absence of a single parameterisation for the deposition velocity as a function of aerodynamic parameters for smooth or rough surfaces. This absence is certainly due to the lack of reported data with turbulent parameters and the lack of deposition experiments on rough walls, even for simple roughness geometries. In the case of pollution by radionuclides, the disparity in the deposition velocities about two orders of magnitude measured in this study shows the importance of a local estimate of depositions in the urban canopy for each surface, rather than an estimate on the scale of entire neighbourhoods. Finally, a wind tunnel study can only constitute a first step in studying dry deposition in the urban environment and should be supplemented by *in situ* measurements.

V. REFERENCES

Antonia R. A., Luxton R. E., 1971. The response of a turbulent boundary layer to a step change in surface roughness, part 1. Smooth to rough. Journal of Fluid Mechanics 48, 721-761.

Chamberlain A.C., 1967. Transport of Lycopodium spores and other small particles to rough surfaces. Proceedings of the Royal Society London, 296 A.

Dai W., Davidson C.I., Etyemezian V., Zufall M., 2001. Wind tunnel studies of particles transport and deposition in turbulent boundary flows. Aerosol Science and Technology 35, 887-898.

348 Damay P., 2010. Détermination expérimentale de la vitesse de dépôt sec des aérosols submicroniques
349 en milieu naturel: influence de la granulométrie, des paramètres micrométéorologiques et du couvert.
350 Thèse de doctorat de l'INSA de Rouen.

351 Donateo A., Damay P. E., Contini D., Maro D., Roupsard P., 2010. Similarities and differences in dry
352 deposition velocity normalized to friction velocity over maize, grass, bare soil and ice measured with
353 different instruments. International Aerosol Conference 2010, Helsinki.

354 Flori J.P., Giraud D., Olive F., Ruot B., Sini J.F, Rosant J.M., Mestayer P., Connan O., Maro D., Hébert
355 D., Rozet M., Talbaut M., Coppalle A., 2007. Salissures de façades (SALIFA), Programme PRIMEQUAL,
356 rapport final. EN-CAPE 07.129 C.

357 Fowler D., Pilegaard K., Sutton M.A., Ambus P., Raivonen M., Duyzer J., Simpson D., Fagerli H., Fuzzi
358 S., Schjoerring J.K., Granier C., Neftel A., Isaksen I.S.A., Laj P., Maione M., Monks P.S., Bukhardt J.,
359 Daemmgen U., Neirynck J., Personne E., Wichink-Kruit R., Butterbach-Bahl K., Flechard C., Tuovinen
360 J.P., Coyle M., Gerosa G., Loubet B., Altimir N., Gruenhage L., Ammann C., Cieslik S., Paoletti E.,
361 Mikkelsen T.N., Ro-Poulsen H., Cellier P., Cape J.N., Horváth L., Loreto F., Niinemets U., Palmer P.I.,
362 Rinne J., Misztal P., Nemitz E., Nilsson D., Pryor S., Gallagher M.W., Vesala T., Skiba U., Brüggemann
363 N., Zechmeister-Boltenstern S., Williams J., O'Dowd C., Facchini M.C., de Leeuw G., Flossman A.,
364 Chaumerliac N., Erisman J.W., 2009. Atmospheric composition change: Ecosystems-Atmosphere
365 interactions. Atmospheric Environment 43, 5193-5267.

366 Gründel M., Porstendörfer J., 2004. Differences between the activity size distributions of the different
367 natural radionuclide aerosols in outdoor air. Atmospheric Environment 38, 3723-3728.

368 Horvath H., Pesava P., Toprak S., Aksu R., 1996. Technique for measuring the deposition velocity of
369 particulate matter to building surfaces. The Science of the Total Environment 189/190, 255-258.

370 Jaenicke R., 1988. Aerosol physics and chemistry. In Landolt-Börstein. Numerical data and functional
371 relationships in science and technology, Group V, Vol. 4 Meteorology, subvolume b Physical and
372 chemical properties of the air. Springer-Verlag, Berlin.

373 Kelly G.N., 1987. The importance of the urban environments for accident consequences. Radiation
374 Protection Dosimetry 21, 13-20.

375 Krogstad P.Å., Antonia R.A., 1999. Surface roughness effects in turbulent boundary layers. Experiments
376 in fluids 27, 450-460.

377 Lai A.C.K., Nazaroff W.W., 2000. Modeling indoor particle deposition from turbulent flow onto smooth
378 surfaces. Journal of Aerosol Science 31, 463-476.

379 Liu B. Y. H., Agarwal J. K., 1974. Experimental observation of aerosol deposition in turbulent flow.
380 Aerosol Science 5, 145-155.

381 Maro, D., Connan, O., Hébert, D., Rozet, M., Talbaut, M., Coppalle, A., Sini, J.F., Rosant, J.M., Mestayer,
382 P., Sacré, C., Flori, J.P., Giraud, D., Olive, F., Ruot, B., Roupsard, P., 2010. Quantification of the dry
383 deposition of aerosols in an urban environment: towards a new methodology. International Aerosol
384 Conference 2010, Helsinki.

385 NF X 44-011, 1972. Séparateurs aérauliques. Méthode de mesure de l'efficacité des filtres au moyen
386 d'un aérosol d'uranine (fluorescéine). AFNOR, La Plaine Saint-Denis.

387 Papastefanou C., 2006. Residence time of tropospheric aerosols in association with radioactive nuclides.
388 Applied Radiations and Isotopes 64, 93-100.

389 Papastefanou C., 2008. Radioactivity in the Environment, Volume 12, Chapter 1, Atmospheric Aerosol
390 Particles. Elsevier Science, Oxford.

391 Pesava P., Aksu R., Toprak S., Horvath H., Seidl S., 1999. Dry deposition of particles to building surfaces
392 and soiling. The Science of the Total Environment 235, 25-35.

393 Petroff A., Mailliat A., Amielh M, Anselmet F., 2008. Aerosol dry deposition on vegetative canopies. Part
394 II: a new modelling approach and applications. Atmospheric Environment 42, 3654-3683.

395 Raupach M. R., Antonia R. A., Rajagopalan S., 1991. Rough-wall turbulent boundary layers. Applied
396 Mechanics Reviews 44, 1-25.

397 Roed J., 1983. Deposition velocity of caesium-137 on vertical building surfaces. Short Communication,
398 Atmospheric Environment 17, 663-664.

399 Roed J., 1985. Dry deposition of urban surfaces. Risø-R-515 NKA/REK-1(84)701, Risø National
400 Laboratory, Roskilde.

401 Roed J., 1987. Dry deposition in rural and in urban areas in Denmark. Radiation Protection Dosimetry 21,
402 33-36.

403 Schlichting H., 1968. Boundary-Layer Theory. McGraw Hill, New York.

404 Sehmel G.A., 1980. Particle and gas dry deposition: a Review. Atmospheric Environment 14, 983-1011.

405 Toprak S., Aksu R., Pesava P., Horvath H., 1997. The soiling of materials under simulated atmospheric
406 conditions in a wind tunnel. Journal of Aerosol Science 28, Supplement 1, S585-S586.

407 Van Dingenen R., Raes F., Putaud J.P., Baltensperger U., Charron A., Facchini M.-C., Decesari S., Fuzzi
408 S., Gehrig R., Hansson H.-C., Harrison R.M., Hüglin C., Jones A.M., Laj P., Lorbeer G., Maenhaut W.,
409 Palmgren F., Querol X., Rodriguez S., Schneider J., ten Brink H., Tunved P., Tørseth K., Wehner B.,
410 Weingartner E., Wiedensohler A., Wåhlin P., 2004. A European aerosol phenomenology – 1: physical
411 characteristics of particulate matter at kerbside, urban, rural and background sites in Europe.
412 Atmospheric Environment 38, 2561-2577.

413 Zhang L., Gong S., Padro J., Barrie L., 2001. A size-segregated particle dry deposition scheme for an
414 atmospheric aerosol module. Atmospheric Environment 35, 549-560.

Figures

Click here to view linked References

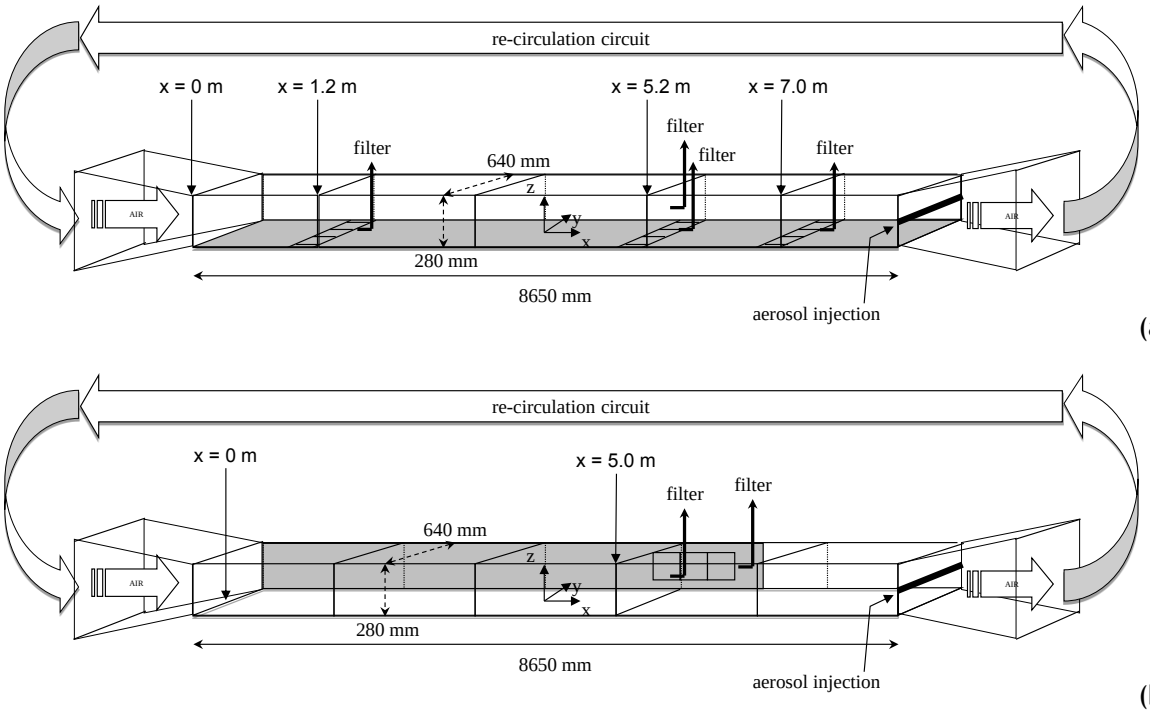

Fig. 1: illustrations of the wind tunnel configurations to study deposition on horizontal (a) and vertical (b) walls; the studied surface is grey; the substrates samples are the grey squares.

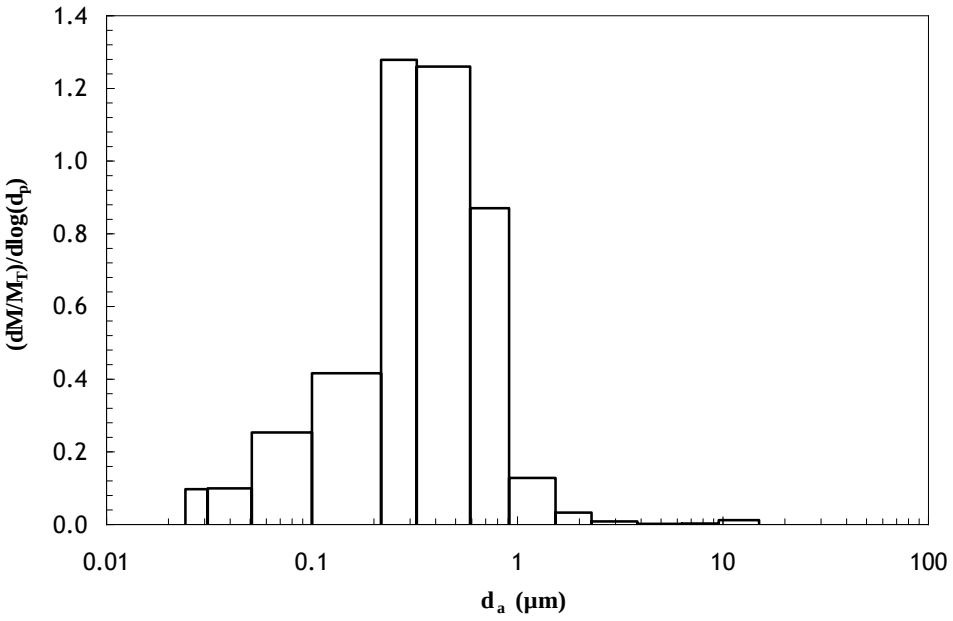

Fig. 2: normalised granulometric mass distribution of the fluorescein aerosol.

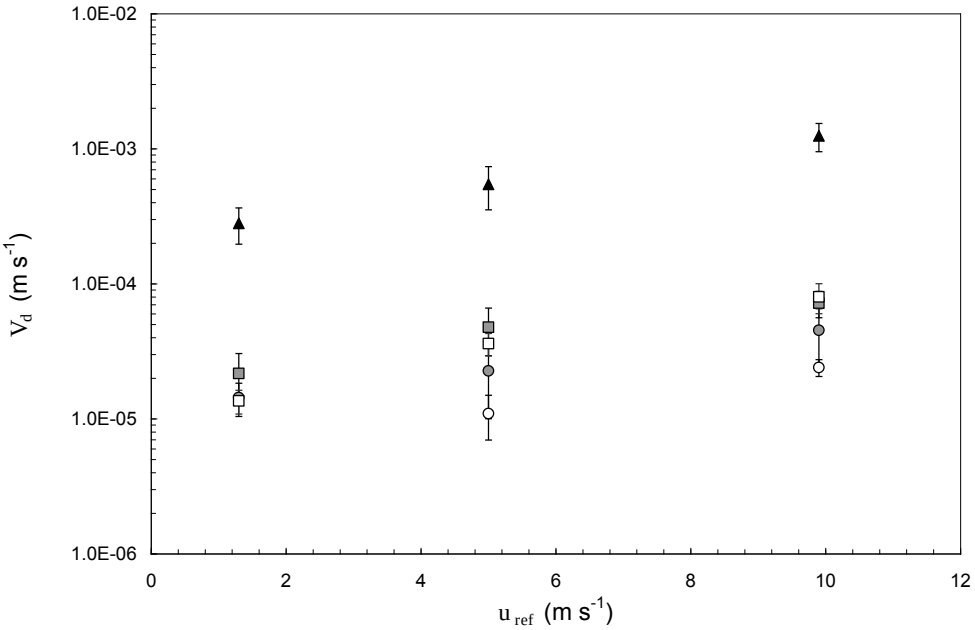

Fig. 3: average V_d as a function of u_{ref}.

● Horizontal conventional glass; ○ Vertical conventional glass;

■ Horizontal cement facing; □ Vertical cement facing;

▲ Synthetic grass.

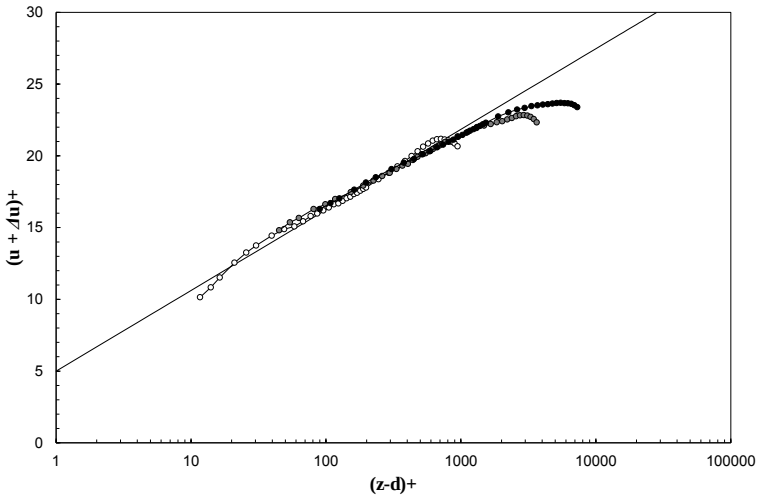

a)

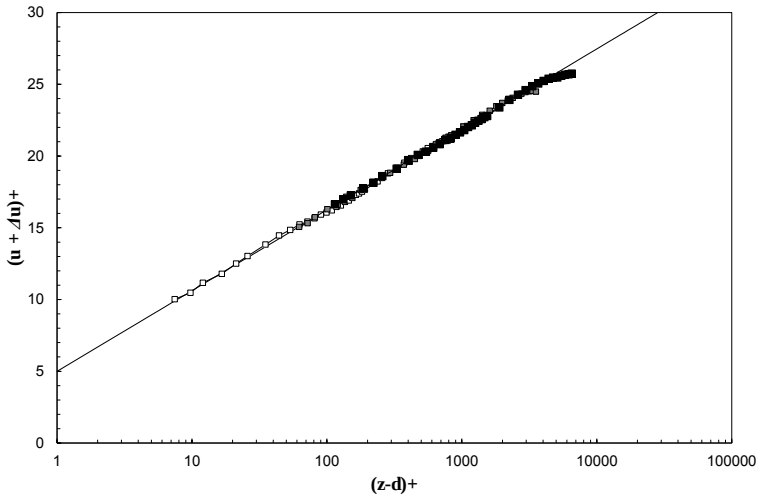

b)

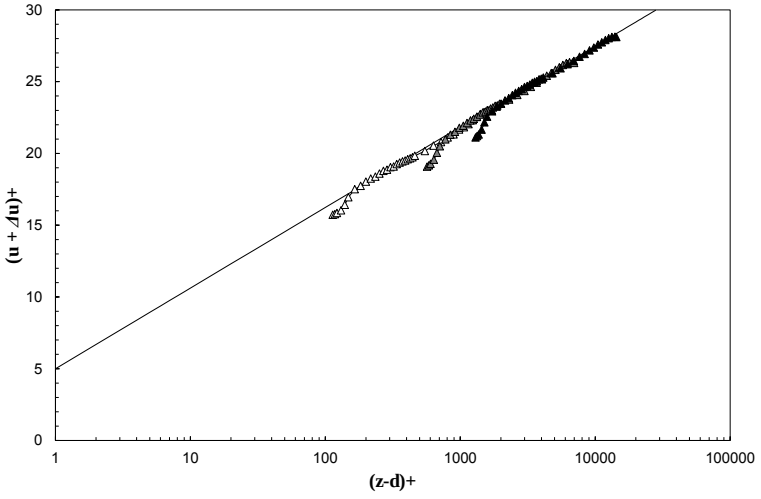

c)

Fig. 4: $u+$ as a function of $z+$ for a fetch of 5.10 m for each type of surface and each u_{ref}.

a) Conventional glass: ○ u_{ref} = 1.3 m s^{-1}; ● u_{ref} = 5.0 m s^{-1}; ● u_{ref} = 9.9 m s^{-1};

b) Cement facing: □ u_{ref} = 1.3 m s^{-1}; ■ u_{ref} = 5.0 m s^{-1}; ■ u_{ref} = 9.9 m s^{-1};

c) Synthetic grass: △ u_{ref} = 1.3 m s^{-1}; ▲ u_{ref} = 5.0 m s^{-1}; ▲ u_{ref} = 9.9 m s^{-1}.

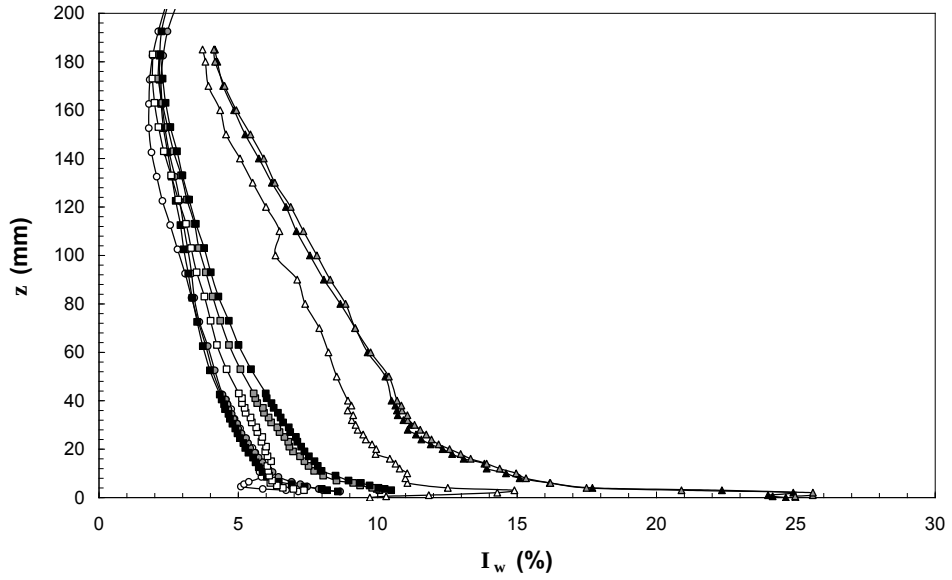

Fig. 5: I_w as a function of z for a fetch of 5.10 m, for each surface type and each u_{ref}.

Conventional glass: ○ u_{ref} = 1.3 m s^{-1}; ◍ u_{ref} = 5.0 m s^{-1}; ● u_{ref} = 9.9 m s^{-1};

Cement facing: □ u_{ref} = 1.3 m s^{-1}; ▣ u_{ref} = 5.0 m s^{-1}; ■ u_{ref} = 9.9 m s^{-1};

Synthetic grass: △ u_{ref} = 1.3 m s^{-1}; ▲ u_{ref} = 5.0 m s^{-1}; ▲ u_{ref} = 9.9 m s^{-1}.

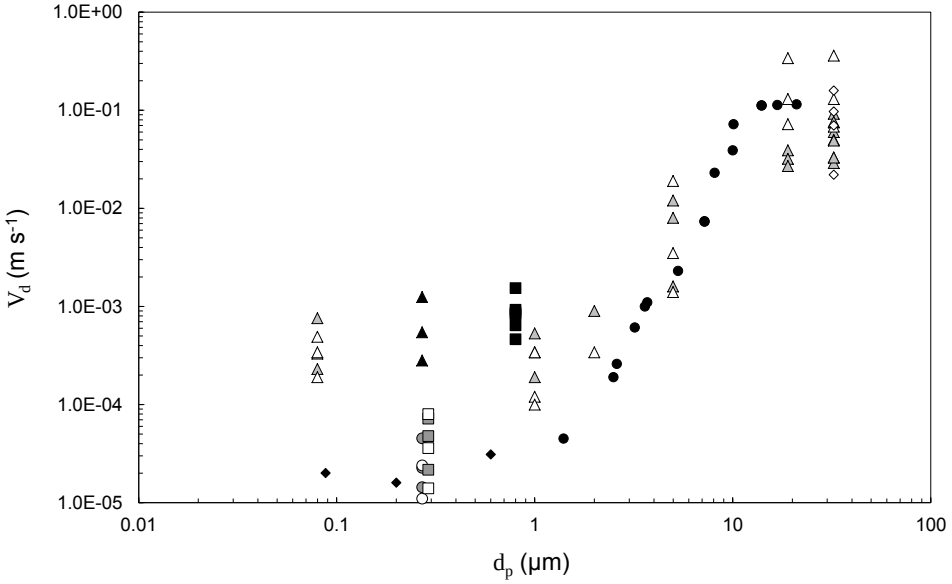

Fig. 6: mean V_d of this study and V_d from the literature as a function of d_p.

● Vertical glass (Liu and Agarwal, 1974); ◆ Glass (Horvath *et al.* ,1996); ◇ horizontal sticky rough glass (Chamberlain, 1967); ■ Cement (Toprak *et al.*, 1997); △ Sticky artificial grass, ▲ Real grass (Chamberlain, 1967);

This study: ◍ Horizontal conventional glass; ○ Vertical conventional glass;

▣ Horizontal cement facing; □ Vertical cement facing;

▲ Synthetic grass.

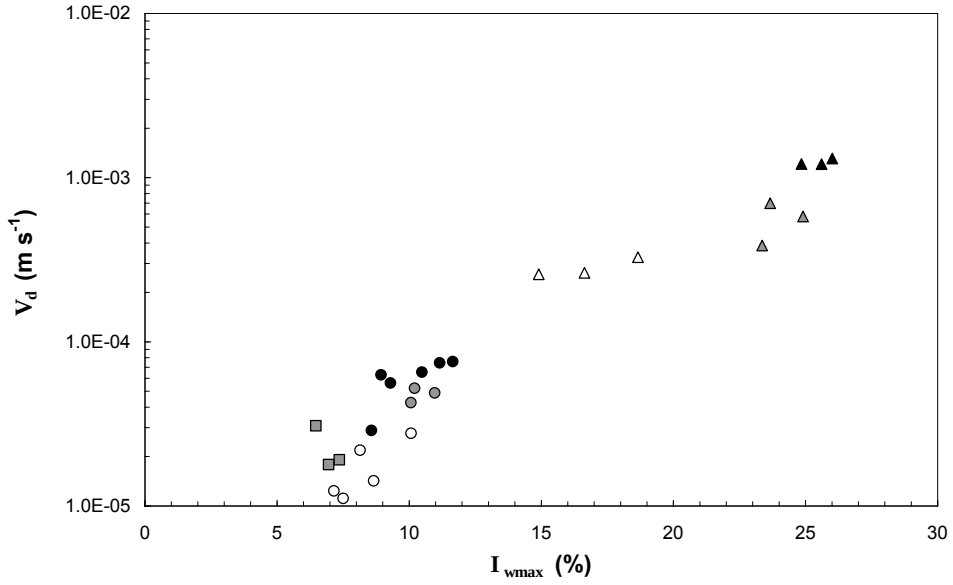

Fig. 7: average V_d as a function of I_{wmax} for each type of surface.

Conventional glass: ○ u_{ref} = 1.3 m s^{-1}; ● u_{ref} = 5.0 m s^{-1}; ● u_{ref} = 9.9 m s^{-1};

Cement facing: □ u_{ref} = 1.3 m s^{-1}; ■ u_{ref} = 5.0 m s^{-1}; ■ u_{ref} = 9.9 m s^{-1};

Synthetic grass: △ u_{ref} = 1.3 m s^{-1}; ▲ u_{ref} = 5.0 m s^{-1}; ▲ u_{ref} = 9.9 m s^{-1}.

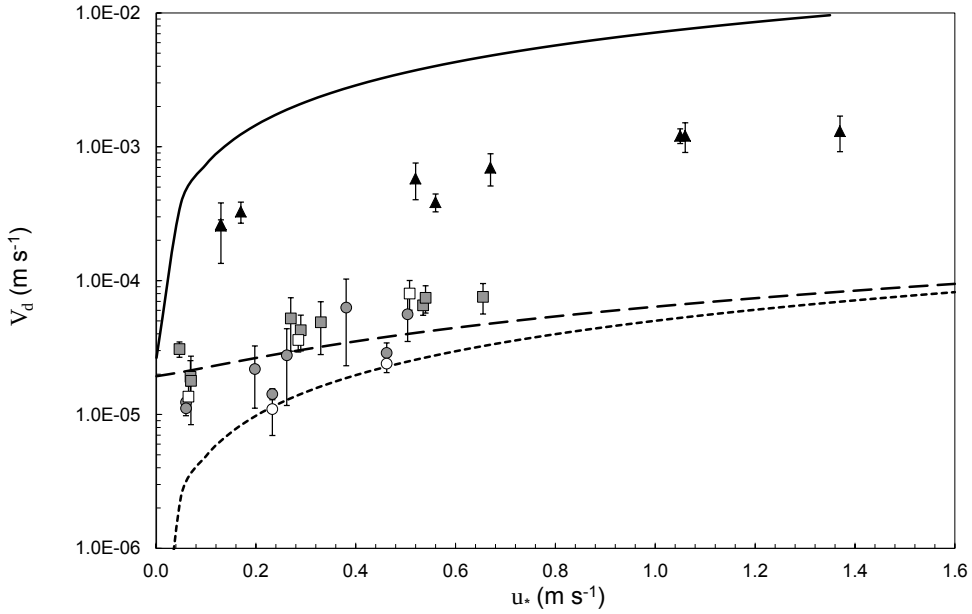

Fig. 8: V_d as a function of u_*, comparison of model to measurements.

– – – Horizontal smooth wall, - - - Vertical smooth wall (Lai and Nazaroff, 2000);

—— Grass (Zhang *et al.*, 2001);

This study: ● Horizontal conventional glass; ○ Vertical conventional glass;

■ Horizontal cement facing; □ Vertical cement facing;

▲ Synthetic grass.

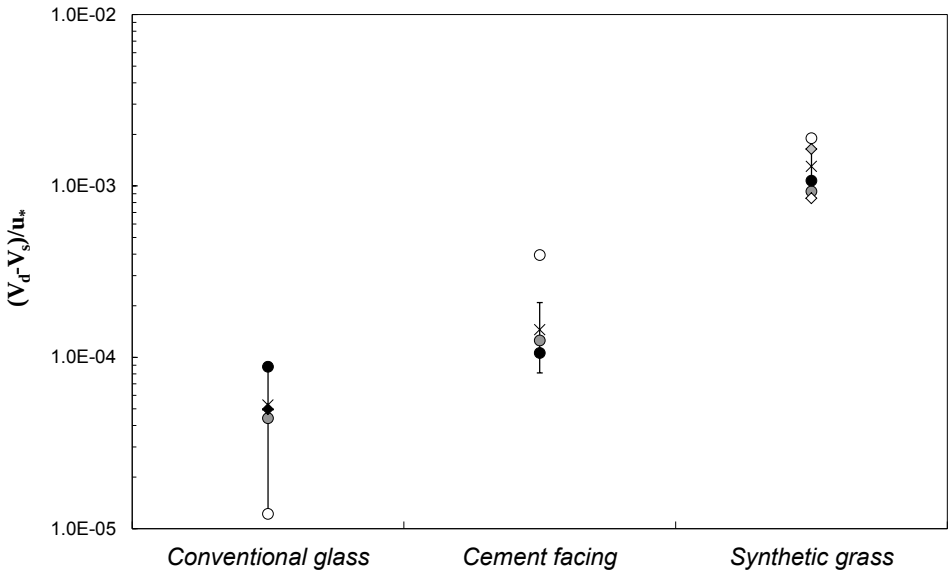

59

60 Fig. 9: $\frac{V_d - V_s}{u_*}$ ratios for each type of horizontal surface.

61 ◆ Smooth wall (Lai and Nazaroff, 2000);

62 ◇ Grass (d_p = 0.202 μm), ◈ Grass (d_p = 0.316 μm) (Damay, 2010);

63 This study: ○ u_{ref} = 1.3 m s^{-1}; ◍ u_{ref} = 5.0 m s^{-1}; ● u_{ref} = 9.9 m s^{-1}; x mean on all u_{ref} for each surface.